# Multi-operator Based Signal Separation Approach

Baokui Guo, Silong Peng, Xiyuan Hu
Institute of Automation
Chinese Academy of Sciences
Beijing 100190, China
{guobaokui2014, silong.peng, xiyuan.hu}@ia.ac.cn

Pengcheng Xu
Academy of Mathematics and Systems Science
Chinese Academy of Sciences
Beijing 100190, China
xupc@amss.ac.cn

***Abstract*—The null space pursuit (NSP) algorithm is an operator-based signal separation approach which separates a signal into a set of additive subcomponents using adaptively estimated operators. In this paper, we introduce a multi-operator based strategy and propose multi-operator based null space pursuit (MONSP) algorithm for signal separation. On the one hand, the proposed approach is a generalized formulation of the original work in some sense. On the other hand, compared with the NSP, the proposed approach has its intrinsic advantages: 1), the proposed approach avoids the mode-mixing problems which is often meet in NSP algorithm; 2), the multi-operator based formulation could theoretically reach the ideal separation resolution for the noise-free signal separation; 3), the MONSP algorithm does not need to initialize parameters in each iteration. We perform several experiments on synthetic and real-life signal separation by MONSP and compare some results with the state-of-the-art methods to demonstrate the efficiency and robustness of the proposed method.**

***Index Terms*—Signal separation, null space pursuit, multi-operator based approach, empirical mode decomposition, amplitude-modulated and frequency-modulated signal.**

## I. Introduction

In recent years, many approaches have been proposed to separate a signal into a set of additive subcomponents [1]-[11]. The separation methods are categorized as three groups: 1) the time-frequency analysis methods, e.g. short-time Fourier transform, wavelet transform, time-frequency reassignment [1], [2], Synchrosqueezing wavelet transform (SWT) [3], [4] etc; 2) data-driven adaptive method, e.g. empirical mode decomposition [5], ensemble empirical mode decomposition (EEMD) [6] etc; 3) optimization-based method, e.g. sparsity based method [7], [8], operator-based method [9], [10], [11] etc. The operator-based signal separation (OSS) approach proposed by Peng et al. [9] separates a signal $S$ into subcomponent $U$ and a residual signal $R$ so that $S = U + R$ and $U$ is in the null space of an operator $\mathcal{T}_S$. The operator $\mathcal{T}_S$ is usually characterized by some parameters that can be estimated from $S$ adaptively. The objective of OSS is to solve the following optimization problem:

$$\min_{U}\{\|\mathcal{T}_S U\|^2 + \lambda\|\mathcal{H}(S-U)\|^2\}, \tag{1}$$

where $S-U$ is the residual signal and $\mathcal{H}$ is an identical or differential operator that regularizes $S-U$. Minimizing $\|\mathcal{T}_S U\|^2$ indicates that the extracted signal $U$ is in the null space of an adaptive operator $\mathcal{T}_S$. The optimal solution of (1) is:

$$\hat{U}(t) = (\mathcal{T}_S^*\mathcal{T}_S + \lambda\mathcal{H}^*\mathcal{H})^{-1}\lambda\mathcal{H}^*\mathcal{H}S(t), \tag{2}$$

where $(\cdot)^*$ is the conjugation of operators. The separation result by OSS approach is sensitive to $\lambda$ since different value of $\lambda$ results in different solution (2).

In order to improve the robustness and effectiveness of OSS approach, Peng and Hwang [10] introduced a leakage term and proposed the null space pursuit (NSP) algorithm. It is to optimize the following problem:

$$\min_{U,\mathcal{T}}\{\|\mathcal{T}(U)\|_2^2 + \lambda(\|(S-U)\|_2^2 + \gamma\|U\|_2^2) + \mathcal{F}(\mathcal{T}_U)\}. \tag{3}$$

The first term and second term correspond to the two terms in (1); the third term called leakage term determines the amount of $U$ to be retained in the null space of $\mathcal{T}$, which makes the optimization less greedy and more robust; and the last term $\mathcal{F}(\mathcal{T}_U)$ is a Lagrange term for regularizing the operator parameter. The NSP algorithm optimizes $\mathcal{T}$ and signal $U$ in (3) alternatively, and based on some assumptions, the parameters $\lambda$ and $\gamma$ are updated in each iteration [10], [12].

The most widely used operator in OSS approach and NSP is the differential operator [10]:

$$\mathcal{T} = \frac{d^2}{dt^2} + \alpha(t), \tag{4}$$

where parameter $\alpha(t)$ is a second-order continuously differentiable function. For a signal $U(t) = A(t)\cos(\phi(t))$, if $\alpha(t) = \phi'^2(t)$, then$\mathcal{T}(U(t)) \approx 0$ if $A(t)$ and $\phi'(t)$ are slow-varying functions.

The residual signal $S-U$ can be iteratively separated by NSP algorithm and by separating residuals iteratively for $K$ times, the input signal can be separated into $K$ subcomponents plus a residual signal as

$$S = \sum_{i=1}^{K} U_i + R, \tag{5}$$

where $U_i$ is the $i$-th extracted subcomponent signal, each of which is in the null space of an adaptive operator, and $R$ is the ultimate residual signal.

In this paper, we utilize a multi-operator based strategy for signal separation and propose a multi-operator based null space pursuit algorithm (MONSP). This approach is an one-shot method which extracts all components at the same time instead of extracting components sequentially. Compared

978-1-5090-4165-7/16/$31.00 ©2016 IEEE

with the single-operator form (1) and (3), the multi-operator based method 1) avoids mode-mixing problems; 2) could theoretically reach the ideal separation resolution if the input signal is noise free; 3) does not need to reset initial values of the parameters $\lambda$ and $\gamma$ in (3). We present this approach in section II and demonstrate the performance of the proposed approach by some separation experiments on synthetic and real-life signals in section III.

## II. Multi-operator Based Signal Separation

The objective of multi-operator based signal separation (MOSS) approach is to separate a multi-component signal into sum of several mono-component signals and a residual noise by using multiple operators. In this section, we first give the signal model and then derive the MOSS approach, and lastly propose the multi-operator based null space pursuit (MONSP) algorithm for discrete signal separation.

### A. Signal Model

In this paper, a *mono-component* signal is defined as an amplitude-modulated and frequency-modulated (AM-FM) signal:

$$U(t) = A(t)\cos(\phi(t)), \tag{6}$$

where $A(t)$ and $\phi(t)$ represent the instantaneous amplitude (IA) and the instantaneous phase (IF), respectively. Generally, both the IA $A(t)$ and instantaneous frequency (IF) $\phi'(t)$ are slow-varying functions. A *multi-component* signal can be represented as

$$S(t) = \sum_{i=1}^{K} A_i(t)\cos(\phi_i(t)) + R(t), \tag{7}$$

where $K$ is the number of mono-components and $R(t)$ is noise, e.g. Gaussian noise.

### B. Multi-operator Based Approach

For a multi-component signal $S(t) = \sum_{i=1}^{K} U_i(t) + R(t) = \sum_{i=1}^{K} A_i(t)\cos(\phi_i(t)) + R(t)$, if $\mathcal{T}_i = d^2/dt^2 + \phi_i'^2(t)$ $(i = 1, 2, ..., K)$, then each subcomponent $A_i(t)\cos(\phi_i(t))$ is approximately in the null space $\mathcal{T}_i$ since $\mathcal{T}_i U_i(t) \approx 0$.

Denote $\mathcal{D}$ as the second differential operator, i.e. $\mathcal{D}S(t) = S''(t)$. Then given a component number $K$, the multi-operator based approach for separating multi-component signal $S(t)$ is to optimizing the following problem:

$$\hat{U}_i, \hat{\mathcal{T}}_i (i = 1, 2, ..., K) = \underset{U_i, \mathcal{T}_i (i=1,...,K)}{\operatorname{argmin}} \{\sum_{i=1}^{K} \|\mathcal{T}_i(U_i)\|^2 + \lambda \|S - \sum_{i=1}^{K} U_i\|^2 + \mathcal{F}(\mathcal{T}_1, \cdots, \mathcal{T}_K)\}, \tag{8}$$

where $U_i$ $(i = 1, 2, ..., k)$ is the subcomponents to be extracted and $\mathcal{T}_i = \mathcal{D} + \alpha_i(t)$ is the associated operator. The parameter $\alpha_i(t)$ in $\mathcal{T}_i$ is unknown and needs to be optimized. The last term $\mathcal{F}(\mathcal{T}_1, \cdots, \mathcal{T}_K)$ is a regularization term which regulates these operators. Generally, $\mathcal{F}(\mathcal{T}_1, \cdots, \mathcal{T}_K) = \gamma \sum_{i=1}^{K} \|\mathcal{D}\alpha_i(t)\|^2$, which ensures the smoothness of each parameter $\alpha_i(t)$. With the optimal solution $\hat{U}_i$ and $\hat{\mathcal{T}}_i$ ($\hat{\mathcal{T}}_i = \mathcal{D} + \hat{\alpha}_i(t)$) of (8), the multi-component signal $S(t)$ can be represented as a sum of subcomponents and a residual signal as (7), that is $S(t) = \sum_{i=1}^{K} \hat{U}_i(t) + R(t)$. Each component $\hat{U}_i(t)$ is in the null space of $\hat{\mathcal{T}}_i$, whose parameter $\hat{\alpha}_i(t)$ is equal to the square of IF of $\hat{U}_i(t)$. We will derive an algorithm termed multi-operator based null space pursuit (MONSP) to solve (8) in section II-C.

In fact, other operators, such as AM-FM operator $d^2/dt^2 + P(t)d/dt + Q(t)$ [12], integral operator [11], etc., can also be utilized in the proposed method. There will be similar results in our approach with other formations of operator, thus we will just use the differential operator (4) in the discussion.

### C. Multi-operator Based Null Space Pursuit Algorithm

We use the upper and the bold lower case, e.g. $T$ and $\boldsymbol{s}$, to represent a matrix and discrete signal respectively in the following.

In discrete case, the parameter $\alpha$ in operator (4) is corresponding to discrete signal $\boldsymbol{\alpha}(n)$ and the differential operator denoted as $T$, has the form:

$$T = D + A_{\boldsymbol{\alpha}}, \tag{9}$$

where $D$ is the second difference matrix, i.e. $D\boldsymbol{s}(n) = \boldsymbol{s}(n+1) - 2\boldsymbol{s}(n) + \boldsymbol{s}(n-1)$, and $A_{\boldsymbol{\alpha}}$ is a diagonal matrix whose diagonal elements are equal to $\boldsymbol{\alpha}$.

Denote

$$F(\boldsymbol{u}_i, \boldsymbol{\alpha}_i : i = 1, ..., K) = \sum_{i=1}^{K} \|T_i(\boldsymbol{u}_i)\|^2 + \lambda \|\boldsymbol{s} - \sum_{i=1}^{K} \boldsymbol{u}_i\|^2 + \gamma \sum_{i=1}^{K} \|D(\boldsymbol{\alpha}_i)\|^2. \tag{10}$$

Then the discrete case of (8) is:

$$\hat{\boldsymbol{u}}_i, \hat{T}_i = \underset{\boldsymbol{u}_i, \boldsymbol{\alpha}_i : i=1,...,K}{\operatorname{argmin}} F(\boldsymbol{u}_i, \boldsymbol{\alpha}_i : i = 1, ..., K). \tag{11}$$

The partial derivative to $\boldsymbol{\alpha}_i$ $(i = 1, \cdots, K)$ is

$$\frac{\partial F}{\partial \boldsymbol{\alpha}_i} = 2A_{\boldsymbol{u}_i}^T (A_{\boldsymbol{u}_i}\boldsymbol{\alpha}_i + D\boldsymbol{u}_i) + 2\gamma D^T D\boldsymbol{\alpha}_i, \tag{12}$$

where $(\cdot)^T$ is the transposition of a matrix. So the parameter $\boldsymbol{\alpha}_i$ can be estimated by:

$$\hat{\boldsymbol{\alpha}}_i = -(A_{\boldsymbol{u}_i}^T A_{\boldsymbol{u}_i} + \gamma D^T D)^{-1} A_{\boldsymbol{u}_i}^T D\boldsymbol{u}_i. \tag{13}$$

Similarly, for each subcomponent $\boldsymbol{u}_i$ $(i = 1, \cdots, K)$, the estimation of $\hat{\boldsymbol{u}}_i$ can be obtained by $\partial F/\partial \boldsymbol{u}_i = 0$:

$$\hat{\boldsymbol{u}}_i = \lambda({T_i}^T T_i + \lambda I)^{-1}(\boldsymbol{s} - \sum_{j \neq i} \boldsymbol{u}_j). \tag{14}$$

In fact, the third term of (10) ensures smoothness of operator parameter. Thus we usually estimate the operator parameter $\boldsymbol{\alpha}_i$ by least square method and then post-process $\boldsymbol{\alpha}_i$ with a low-pass filter. That is:

$$\widetilde{\boldsymbol{\alpha}}_i = -(A_{\boldsymbol{u}_i}^T A_{\boldsymbol{u}_i})^{-1} A_{\boldsymbol{u}_i}^T D\boldsymbol{u}_i, \tag{15}$$

$$\hat{\boldsymbol{\alpha}}_i = \widetilde{\boldsymbol{\alpha}}_i \star \boldsymbol{h}, \tag{16}$$

where $(\star)$ is convolution operator and $\boldsymbol{h}$ is a low-pass filter.

Given a multi-component signal $\boldsymbol{s}$ and the component number K, optimization (11) can be solved with (14), (15), (16) by alternating minimization [13]. The procedure denoted as MONSP algorithm is depicted in algorithm 1.

The component number $K$ and the initial value of parameters $\boldsymbol{\alpha}_i$ $(i = 1, 2, ..., K)$ can be obtained by time-frequency distribution (TFD) based ridge detection [14], i.e., the component number $K$ is given by the ridge number of the TFD while the initial $\boldsymbol{\alpha}_i$ is given by the square of each ridge.

**Algorithm 1** MO-NSP

**Input:**

$\lambda$; Stopping threshold $\epsilon$; Stopping iterations $J$; $j = 1$;
The initial values of parameter $\boldsymbol{\alpha}_i^{(0)}$ $(T_i^{(0)} = D + A_{\boldsymbol{\alpha}_i^{(0)}})$, $i = 1, 2, \cdots, K$;

**Loop:**

1: for i = 1 to K do:
$\boldsymbol{u}_i^{(j)} \leftarrow \lambda(T_i^{(j-1)^T} T_i^{(j-1)} + \lambda I)^{-1}(\boldsymbol{s} - \sum_{k \neq i} \boldsymbol{u}_k^{(j-1)})$
end for;

2: for i = 1 to K do:
$\boldsymbol{\alpha}_i^{(j)} \leftarrow -(A^T_{\boldsymbol{u}_i^{(j)}} A_{\boldsymbol{u}_i^{(j)}})^{-1} A^T_{\boldsymbol{u}_i^{(j)}} D \boldsymbol{u}_i^{(j)}$
$\boldsymbol{\alpha}_i^{(j)} \leftarrow \boldsymbol{\alpha}_i^{(j)} \star \boldsymbol{h}$
end for;

3: for i = 1 to K do:
$T_i^{(j)} \leftarrow D + A_{\boldsymbol{\alpha}_i^{(j)}}$ end for;

4: Check if $\sum_{i=1}^{K} \|\boldsymbol{u}_i^{(j+1)} - \boldsymbol{u}_i^{(j)}\|^2 < \epsilon \|\boldsymbol{s}\|^2$ or $j > J$. If so, skip this loop, else $j \leftarrow j + 1$, execute continuously.

**Return:** $\hat{\boldsymbol{u}}_i = \boldsymbol{u}_i^{(j)}$ $(i = 1, 2, \cdots, K)$.

### *D. Comparison with Original Work*

When component number $K$ is set to 1, the problem (8) is identical to (1). Thus this approach is a generalized form in some sense. However, there are still some advantages by using the multi-operator approach for signal separation.

Firstly, the multi-operator based approach solves the mode-mixing problem encountered by single-operator based approach. For example, for a signal $S(t)$ composed of two component $S_i(t) = A_i(t)\cos(f_i t)$ $(i = 1, 2)$, the first extracted signal $\hat{U}(t)$ by (1) or (3) may be a mixture of $S_1(t)$ and $S_2(t)$ such that $\hat{U}(t) = S_1(t)$ when $A_1(t) > A_2(t)$ and $\hat{U}(t) = S_2(t)$ when $A_1(t) < A_2(t)$, since the residual signal $S - U$ in formulation (1) and (3) is constricted with 2-norm. In contrast, when $K = 2$, the optimal solution of (8) is $\hat{U}_i(t) = S_i(t)$ and $\mathcal{T}_i = \mathcal{D} + f_i^2$ $(i = 1, 2)$, which indicates that $S(t)$ is separated perfectly.

Secondly, the MOSS approach can reach the ideal separation of a multi-component signal. For example, $S(t) = U_1(t) + U_2(t) = \cos(f_1 t) + \cos(f_2 t)$. Evidently, the ideal separation resolution are $U_1(t)$ and $U_2(t)$. For the MOSS approach, $U_i$ and $\mathcal{T}_i = \mathcal{D} + f_i^2$ $(i = 1, 2)$ is the optimal solution of (8) since $\mathcal{T}_i U_i = 0$ and $S - U_1 - U_2 = 0$, while the optimal solution of (1) or (3), which is determined by the parameters $\lambda$ and $\gamma$, would not be equal to either $U_1$ or $U_2$.

Lastly, since the original NSP algorithm extracts subcomponent of a signal sequentially, parameters $\lambda$ and $\gamma$ need to be initialized in each iteration which highly affects its robustness, and that will not happen in the one-shot MONSP algorithm.

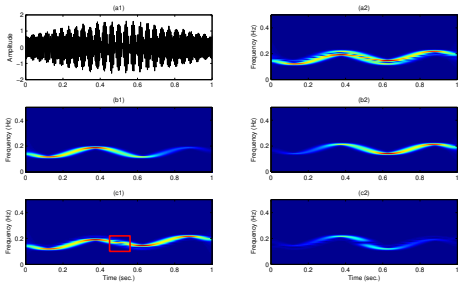


Fig. 1. (a1) signal $S(t)$; (a2) the TFD of $S(t)$; (b1,b2) the TFDs of two extracted subcomponents by MONSP; (c1,c2) the TFDs of the extracted subcomponent and the residual signal by NSP. The SNRs of the two extracted signals by MONSP are 39.1 dB and 38.7 dB respectively. The NSP encounters mode-mixing problem that in the interior of red rectangle, the extracted signal $U_{\text{NSP}}$ is a mixture of $U_1$ and $U_2$; in the left $U_{\text{NSP}}$ is close to $U_1$ and in the right $U_{\text{NSP}}$ is close to $U_2$.

## III. Experiments

In this section, we evaluate the performance of proposed approach through separating several synthetic and real-life signals. Some results are compared with state-of-the-art methods NSP [10], SWT [3], [4] and EEMD [6]. We evaluate the separation results by the signal to noise ratio (SNR) [dB], defined as SNR $= 10\log_{10}(P_s/P_{\text{noise}})$, where $P_s$ and $P_{\text{noise}}$ are the energy of clean signal $s$ and noise respectively. In the following illustration, the short-time Fourier transform [15] based time-frequency distribution (TFD) is used to represent signals. In the following experiments, the parameters $\lambda$ and stopping threshold $\epsilon$ in MONSP are set to $1 \times 10^{-3}$ and $1 \times 10^{-5}$ respectively.

In the first experiment, we consider in time interval [0,1] a signal $S(t)$ composed two mono-components $U_1(t)$ and $U_2(t)$, where $U_1(t) = \exp(-5(t-0.3)^2)\cos(2\pi(160t + 3\cos(2\pi 2t)))$, $U_2(t) = \exp(-5(t-0.7)^2)\cos(2\pi(185t + 3\cos(2\pi 2t)))$. The IFs of these two components are vary close as shown in Fig.1(a2) that makes separation much difficult. It is interesting that $S(t)$ is dominated by $U_1(t)$ in [0,0.5) and by $U_2(t)$ in (0.5,1] since $U_1(t)$ is active around 0.3 while $U_2(t)$ is around 0.7. We use MONSP algorithm with $K = 2$ to separate the discretized signal $S(t)$ (Sampling rate is 1024 Hz). The SNR of the two extracted signals $\hat{U}_1(t)$ and $\hat{U}_2(t)$, corresponding $U_1(t)$ and $U_2(t)$ respectively as shown in Fig.1(b1,b2), are 39.1 dB and 38.7 dB respectively, which indicates that the signal $S(t)$ is well separated. In contrast, the separation result by NSP algorithm is highly affected by mode-mixing problem that the extracted signal is close to $U_1(t)$ in the former period and close to $U_2(t)$ in the latter period as shown in Fig.1(c1,c2).

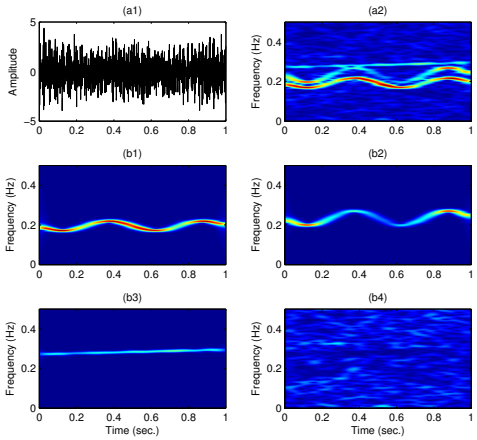


Fig. 2. (a1) the signal $S_\delta(t)$ with $\delta = 0.6$; (a2) the TFDs of $S_\delta(t)$; (b1,b2,b3) the TFDs of three extracted signals from $S_\delta$ by MONSP. (b4) the TFDs of the residual signal.

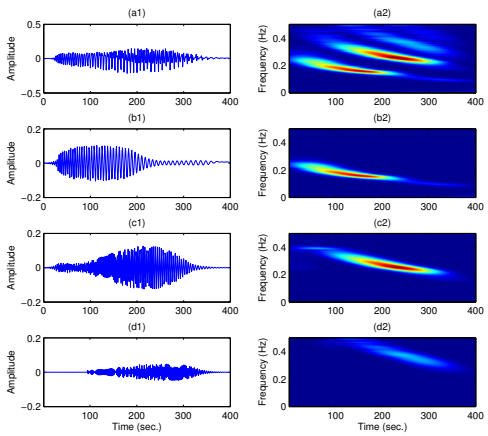


Fig. 3. (a1) the bat signal; (a2) the TFD of the bat signal; (b1,c1,d1) three extracted components from the bat signal by MONSP. (b2,c2,d2) associated TFDs of the three extracted components.

In the second experiment, we try to separate signal $S_\delta(t) = (1.5 + 0.3\cos(2\pi 2t))\cos(2\pi 200t + 4\pi\cos(2\pi 2t)) + (1 + 0.5\cos(2\pi t))\cos(2\pi 240t + 6\pi\cos(2\pi 2t)) + 0.6\cos(2\pi(280t + 12t^2)) + R_\delta(t) \doteq V_1(t) + V_2(t) + V_3(t) + R_\delta(t)$, where $R_\delta(t)$ is the Gaussian noise with variance being $\delta$. Signal $S_\delta(t)$ is contaminated by $R_\delta(t)$ when $\delta$ is big as is illustrated in Fig.2. We use the EEMD, SWT and MONSP with $K = 3$ to separate signal $S_\delta(t)$ with $\delta$ varying from 0.1 to 0.6. The TFDs of three extracted components by MONSP when $\delta = 0.6$ are shown in Fig. 2(b1-b3). From Fig. 2(b1-b4), we can see that the three components $V_i$ $(i = 1, 2, 3)$ are well separated out and the residual signal is nearly contains any information of these three components as its TFD is uniform in the time-frequency plane. More results by MONSP, SWT, and EEMD methods with different values of $\delta$ are shown in Table I ($\text{SNR}_\text{i}$ represents the SNR of the extracted signals which are corresponding to $V_i$ $(i = 1, 2, 3)$ ). We can observe that the MONSP algorithm outperforms other methods since it yields higher SNRs on these noisy signals.

Lastly, in the real-life application, we use the MONSP to separate a bat echolocation call [16] which is available at http://dsp.rice.edu/sites/dsp.rice.edu/files/software/ batsignal.zip. There are 400 samples and the sampling period is 7 $\mu s$. The TFD in Fig.3(a2) shows that the bat signal composes three main components, all of which are nonlinear FM signals and have varying amplitudes. By the MONSP algorithm, the three components are well extracted as shown in Fig. 3(b1,b2,c1,c2,d1,d2).

TABLE I
SNRs OF THREE EXTRACTED SUBCOMPONENTS BY DIFFERENT METHODS FOR SEPARATING $S_\delta(t)$

| Methods\$\delta$ | | 0.1 | 0.2 | 0.3 | 0.4 | 0.5 | 0.6 |
|---|---|---|---|---|---|---|---|
| MONSP | $\text{SNR}_1$ | 29.9 | 27.9 | 25.7 | 23.9 | 22.2 | 20.8 |
| | $\text{SNR}_2$ | 25.6 | 24.3 | 22.5 | 20.9 | 19.4 | 18.1 |
| | $\text{SNR}_3$ | 27.9 | 22.7 | 19.4 | 16.9 | 15.0 | 13.4 |
| SWT | $\text{SNR}_1$ | 19.7 | 19.3 | 18.8 | 18.3 | 17.8 | 17.3 |
| | $\text{SNR}_2$ | 5.71 | 8.52 | 8.52 | 8.48 | 8.25 | 6.71 |
| | $\text{SNR}_3$ | 6.01 | 5.93 | 6.83 | 6.35 | 6.05 | 5.69 |
| EEMD | $\text{SNR}_1$ | 6.98 | 7.06 | 7.18 | 7.32 | 7.47 | 7.62 |
| | $\text{SNR}_2$ | 5.02 | 5.03 | 5.04 | 5.05 | 5.08 | 5.11 |
| | $\text{SNR}_3$ | 0.06 | 0.10 | 0.14 | 0.21 | 0.31 | 0.44 |

## IV. Conclusion

In this paper, we introduce the multi-operator based signal separation (MOSS) strategy and propose the multi-operator based null space pursuit (MONSP) algorithm for signal separation. The MONSP can separate a multi-component signal into sum of several mono-components, each of which is in the null space of an adaptive operator. The proposed approach is in some sense a generalized form of operator-based separation method which utilizes a single operator to separate signals. But the proposed approach has its intrinsic advantages. 1) The MOSS avoids mode-mixing problems when the amplitudes of subcomponents in a multi-component signal are trading off and taking turns; 2) the multi-operator based formulation (8) could reach, whatever the value of $\lambda$ is, the ideal separation resolution theoretically if the input signal is noise free; 3) the MONSP algorithm does not need to initialize the parameters $\lambda$ and $\gamma$ iteratively. The experiments including synthetic and real-life signal separation demonstrate that the proposed method is efficient in multi-component signal separation and robust to the noise.

## Acknowledgment

This work was supported by the Natural Science Foundation of China (61571438).

## REFERENCES


[1] F. Auger, P. Flandrin, Yu-Ting Lin, S. McLaughlin, S. Meignen, T. Oberlin, and Hau tieng Wu, "Time-frequency reassignment and synchrosqueezing:an overview," *IEEE, Signal Processing Magazine*, vol. 30, no. 6, pp. 32–41, 2013.

[2] P. Flandrin, F. Auger, and E. Chassande-Mottin, *Time-frequency reassignment: From principles to algorithms*, Applications in Time-Frequency Signal Processing (A. Papandreou-Suppappola, ed.), ch. 5, 2003.

[3] I. Daubechies, J. F. Lu, and H. T. Wu, "Synchrosqueezed wavelet transforms: An empirical mode decomposition-like tool," *Applied and Computational Harmonic Analysis*, vol. 30, no. 2, pp. 243–261, 2011.

[4] S. Meignen, T. Oberlin, and S. McLaughlin, "A new algorithm for multicomponent signals analysis based on synchrosqueezing: With an application to signal sampling and denoising," *IEEE Transactions on Signal Processing*, vol. 60, no. 11, pp. 5787–5798, 2012.

[5] N. E. Huang, Z. Shen, S. R. Long, M. L. C. Wu, H. H. Shih, Q. N. Zheng, N. C. Yen, C. C. Tung, and H. H. Liu, "The empirical mode decomposition and the hilbert spectrum for nonlinear and non-stationary time series analysis," *Proceedings of the Royal Society a-Mathematical Physical and Engineering Sciences*, vol. 454, no. 1971, pp. 903–995, 1998.

[6] Z. H. Wu and N. E. Huang, "Ensemble empirical mode decomposition: A noise-assisted data analysis method," *Advances in Adaptive Data Analysis*, vol. 01, no. 1, pp. 1–41, 2009.

[7] J. Bobin, J.L. Starck, J.M. Fadili, Y. Moudden, and D.L. Donoho, "Morphological component analysis: an adaptive thresholding strategy," *IEEE Transactions on Image Processing*, vol. 16, pp. 2675–81, 2007.

[8] Ivan W.Selesnick, "Resonance-based signal decomposition: A new sparsity-enabled signal analysis method," *Signal Processing*, vol. 91, pp. 2793–2809, 2011.

[9] S. L. Peng and W. L. Hwang, "Adaptive signal decomposition based on local narrow band signals," *IEEE Transactions on Signal Processing*, vol. 56, no. 7, pp. 2669–2676, 2008.

[10] S. L. Peng and W. L. Hwang, "Null space pursuit: An operator-based approach to adaptive signal separation," *IEEE Transactions on Signal Processing*, vol. 58, no. 5, pp. 2475–2483, 2010.

[11] Hu Xiyuan, Peng Silong, and Hwang Wen-Liang, "Adaptive integral operators for signal separation," *IEEE Signal Processing Letters*, vol. 22, no. 9, pp. 1383–7, 2015.

[12] Xiyuan Hu, Silong Peng, and Wen-Liang Hwang, "Multicomponent am-fm signal separation and demodulation with null space pursuit," *Signal, Image and Video Processing*, vol. 7, no. 6, pp. 1093–1102, 2012.

[13] A. Beck, "On the convergence of alternating minimization for convex programming with applications to iteratively reweighted least squares and decomposition schemes," *Siam Journal on Optimization*, vol. 25, no. 1, pp. 185–209, 2015.

[14] R. A. Carmona, W. L. Hwang, and B. Torresani, "Characterization of signals by the ridges of their wavelet transforms," *IEEE Transactions on Signal Processing*, vol. 45, no. 10, pp. 2586–2590, 1997.

[15] F. Hlawatsch and G. F. Boudreaux-Bartels, "Linear and quadratic time-frequency signal representations," *IEEE Signal Processing Magazine*, vol. 9, no. 2, pp. 21C67, 1992.

[16] R. Baraniuk, "Bat echolocation chirp," *Available: http://dsp.rice.edu/software/bat-echolocation-chirp*.